

CrystEngComm

Accepted Manuscript



This is an *Accepted Manuscript*, which has been through the Royal Society of Chemistry peer review process and has been accepted for publication.

Accepted Manuscripts are published online shortly after acceptance, before technical editing, formatting and proof reading. Using this free service, authors can make their results available to the community, in citable form, before we publish the edited article. We will replace this *Accepted Manuscript* with the edited and formatted *Advance Article* as soon as it is available.

You can find more information about *Accepted Manuscripts* in the [Information for Authors](#).

Please note that technical editing may introduce minor changes to the text and/or graphics, which may alter content. The journal's standard [Terms & Conditions](#) and the [Ethical guidelines](#) still apply. In no event shall the Royal Society of Chemistry be held responsible for any errors or omissions in this *Accepted Manuscript* or any consequences arising from the use of any information it contains.

Cite this: DOI: 10.1039/c0xx00000x

www.rsc.org/xxxxxx

ARTICLE TYPE

Ferromagnetic intermolecular exchange interaction in ethynyl-verdazyl radical crystals

Areej Merhi,^a Thierry Roisnel,^a Stéphane Rigaut,^a Cyrille Train^b and Lucie Norel^{a*}

Received (in XXX, XXX) Xth XXXXXXXXX 20XX, Accepted Xth XXXXXXXXX 20XX

DOI: 10.1039/b000000x

An oxoverdazyl radical substituted by *p*-ethynylphenyl has been synthesised and structurally characterized at different temperatures. Single Crystal XRD studies reveal that the radicals form unusual slipped 1D chains held together by π - π interactions. The intermolecular exchange interaction within the chain is ferromagnetic. This rare situation is tentatively related to the relative position of the radicals within the chains.

Introduction

Persistent organic radicals are promising building blocks for either purely organic or metal-radical based functional magnetic materials.¹ In this context, the control of the solid state magnetic properties of such systems, especially of the nature and strength of the intermolecular exchange interaction requires fine tuning of the solid-state organization of the radicals through π -stacking.²⁻⁴ Thanks to the synthetic versatility offered by several classes of radicals such as benzotriazinyls or nitroxides, ferromagnetic intermolecular interactions have been obtained.^{5,6} Intriguingly, in spite of the synthetic versatility of this family of radicals,⁷ verdazyl radicals with ferromagnetic intermolecular interactions are a minority,⁸ with only one structurally characterized compound, namely the 3-(*p*-nitrophenyl)-1,5,6-triphenyl-verdazyl.⁹ Recent theoretical investigations have rationalized the occurrence of strong antiferromagnetic interactions in the majority of oxoverdazyls radicals based solids and have also shown that a careful control of through space interaction could lead to strong ferromagnetic exchange interactions.⁴ In parallel, we have designed 1,5-dimethyl-3-(*p*-phenylethynyl)-6-oxoverdazyl for further incorporation into ruthenium bis-acetylide complexes to achieve redox switches.¹⁰ In this communication, we report the synthesis and the crystallographic study of this organic radical that reveals an original arrangement of the verdazyl molecules in slipped π -stacked columns. The correlation between the structure and the ferromagnetic behaviour observed by magnetometry is discussed.

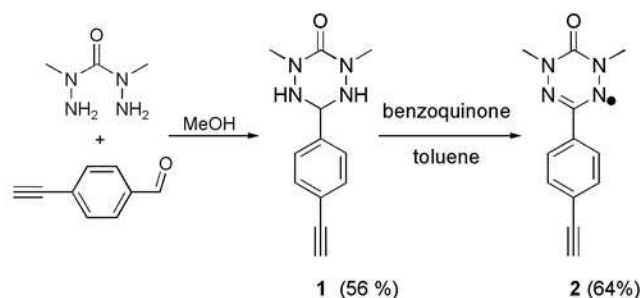
Results and Discussion

Synthesis

The synthesis of 1,5-dimethyl-3-(*p*-ethynylphenyl)-6-oxoverdazyl **2** was achieved by the classical two steps methods involving first the formation of the corresponding tetrazane **1** by reaction of 4-

ethynyl-benzaldehyde and bis(1-methylhydrazide)carbonic acid followed by oxidation with benzoquinone (scheme 1). The infrared spectrum for **2** shows a $\nu(\text{C}=\text{O})$ vibration at 1684 cm^{-1} which is characteristic of the oxo-verdazyl ring. Expected stretchings for the terminal alkyne are found at 2102 cm^{-1} ($\nu(\text{C}\equiv\text{C})$) and 3250 cm^{-1} ($\nu(\text{C}-\text{H})$). Finally, the high frequency infrared spectrum for **2** exhibits vibrations attributed to O-H stretching from water molecules. Indeed, elemental analysis supports the presence of cocrystallization water molecules. In solution characterization was completed with electrochemical and UV-vis absorption studies. Cyclic voltammetry measured in dichloromethane (0.2 M nBu₄NPF₆) shows two monoelectronic waves at 0.33 V ($\Delta E_p = 75\text{ mV}$, $I_a/I_c = 1$) and -1.34 V ($\Delta E_p = 205\text{ mV}$, $I_a/I_c = 0.93$) vs. Cp₂Fe^{0/+} as previously observed in similar oxoverdazyl structures.¹¹ The UV-vis spectrum of **2** showed two transitions at 422 nm ($1800\text{ mol}^{-1}\cdot\text{L}\cdot\text{cm}^{-1}$) and 484 nm ($500\text{ mol}^{-1}\cdot\text{L}\cdot\text{cm}^{-1}$), both with vibronic progression, attesting the rigidity of the structure (Fig. S1). These two bands are typical for oxoverdazyl structures and the low energy transition has been previously assigned to a π (ethynylbenzene) to SOMO (verdazyl) transition.¹¹

Scheme 1



Description of the crystallographic structure

Compound **2** crystallizes by slow evaporation of a dichloromethane solution in the triclinic space group P-1 (Table 1). The unit cell contains two molecules, which are images by the inversion center. After fine analysis of the difference Fourier map, all the hydrogen atoms were included in their calculated positions. The molecular structure at 293 K (Fig. 1) reveals that the verdazyl ring is essentially planar with bond lengths similar to other oxoverdazyl radicals.¹² This ring is almost coplanar with the phenyl ring, the angle between the two mean planes being

7.3°.

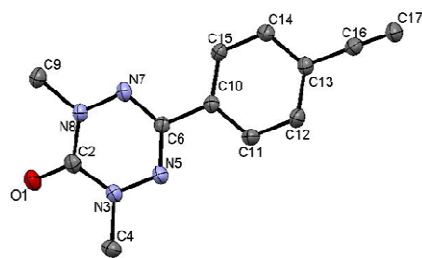


Fig. 1 Thermal ellipsoid plot of radical **2**. Selected bond lengths at 293 K: O(1)-C(2) 1.2190(19), C(2)-N(3) 1.369(2), C(2)-N(8) 1.370(2), N(3)-N(5) 1.3680(19), N(8)-N(7) 1.3647(19), N(7)-C(6) 1.332(2), N(5)-C(6) 1.329(2)

The intermolecular arrangement of the verdazyl rings was then inspected since strong through space exchange interactions can result from close contacts between these radicals.^{2, 3, 13, 14} The molecules stack along the *a* axis, giving rise to columns of radicals (fig. 2a). Within a column, the verdazyl mean planes are parallel, regularly spaced with an inter-radical distance of 3.40 Å. The distance between the verdazyl rings centroids is 4.06 Å and the tilt angle between *a* axis (direction of stacking) and the normal to the verdazyl ring is 33°. The relative location of two neighbouring radical is of peculiar interest: The N-N bonds of the verdazyl moieties are located right above the C-C bonds between the two cycles of neighbouring radicals (Fig. 2b). In the *bc* plane, the radicals are arranged in order to favour a H bond between one alkyne proton and one C=O moiety with $d(\text{C}-\text{O}) = 3.16$ Å (fig. 2c) leading to the formation of straight lines of molecules. Neighbouring lines are running in opposite direction. This alternation of polarized lines with dipole moments orientated in opposite directions is dictated by the minimization of dipolar interactions while the interaction between the successive planes is

governed by π - π interactions. The resulting arrangement of the radicals does not show the usually observed head-over-tail verdazyl stacking but instead an almost ideal parallel displaced stacking leading to slipped 1D chains (fig 2a). In comparison, the structure of 3-(*p*-nitrophenyl)-1,5,6-triphenyl-verdazyl also shows slipped stacks induced by the bulkiness of the phenyl ring on the 6 position which blocks π stacking between the verdazyl moieties.⁹ In these stacks, the distance between successive verdazyl rings is as large as 6.6 Å because the closest contacts are established between one verdazyl ring and the 3-phenyl substituent of another radical. Thus a strategy relying on steric constrain to induce the slippage within the stacks suffers from its tendency to increase radical-radical distance and is unlikely to lead to strong ferromagnetic interaction. On the contrary, the arrangement of molecules **2** is more favourable because the 1,5-dimethyl-6-oxoverdazyl unit is essentially planar.

Intermolecular exchange interaction can be strongly affected by thermally generated intermolecular distances changes, sometimes leading to intriguing magnetic behaviour.^{3, 14} We solved the structure of **2** at three easily accessible temperatures (100, 200 and 293 K). This inspection showed significant variations of the crystal structure in this range of temperature (Table 1). Upon lowering the temperature, the *a* parameter is varied from 4.0513(9) to 3.9458(2) Å (-2.6 %) when *b* and *c* parameters are reduced by less than 0.5 %. Because *a* is the direction of the 1D stacks, the interplane separation between the verdazyl radicals goes from 3.40 Å at 293 K to 3.32 Å at 100 K. This variation (-2.3 %) can be compared with the one observed in AF coupled face-to-face dimers,³ for which the calculated exchange interaction is divided by three with a -4.7 % change of the interplane separation. It was thus interesting to evaluate the influence of these structural changes on the magnetic properties.

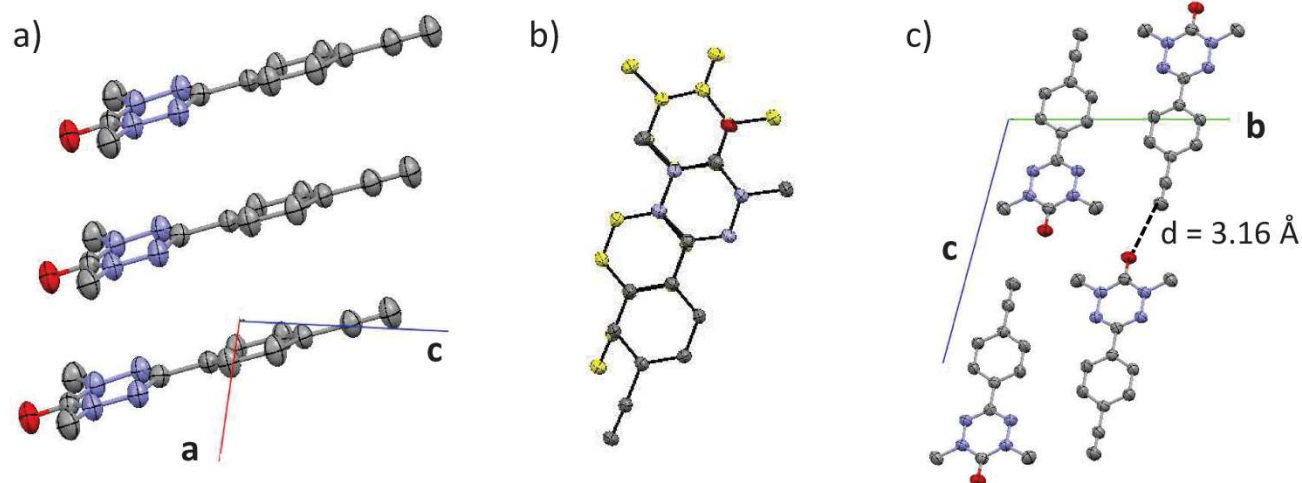


Fig.2 Views of the crystal packing of **2** along the *a* axis (a), perpendicular to the radical plane (b) and in the *bc* plane (c)

60

Cite this: DOI: 10.1039/c0xx00000x

www.rsc.org/xxxxxx

ARTICLE TYPE

Table 1 Crystallographic data and collection parameters for **2**.

Temperature (K)	293	200	100
Empirical formula		C ₁₂ H ₁₁ O ₆ N ₄	
Formula weight		227.25	
Crystal size [mm ³]		0.33 x 0.22 x 0.05	
Color, Habit		red plates	
Crystal system		triclinic	
Space group		P-1	
a [Å]	4.0513(9)	3.9940(4)	3.9458(2)
b [Å]	11.154(2)	11.1412(9)	11.1337(4)
c [Å]	12.902(3)	12.8857(11)	12.8406(5)
α [°]	104.617(11)	104.875(4)	105.091(2)
β [°]	94.207(11)	94.557(4)	95.100(2)
γ [°]	94.195(12)	93.967(4)	93.601(2)
Volume [Å ³]	560.1(2)	550.03(8)	540.32(4)
Z	2	2	2
Θ range [°]	3.72 to 27.48	4.21 to 27.48	3.31 to 27.48
h,	-5/5,	-5/5,	-5/5,
k,	-14/14,	-14/14,	-13/14,
l range	-16/16	-16/16	-16/16
Reflections collected	6796	6715	6599
/independent	/ 2469	/ 2472	/ 2430
Reflections [I > 2σ(I)]	1498	1673	1909
Number of parameters	154	155	155
R ₁ (I > 2σ(I))	0.0537	0.0763	0.047
R ₁ (all)	0.0959	0.0502	0.0609
ωR ₂ (I > 2σ(I))	0.1406	0.1192	0.1207
ωR ₂ (all)	0.1663	0.134	0.1299
Largest diff. peak & hole [e/Å ³]	0.199/ -0.176	0.244 / -0.165	0.383/ -0.208

Magnetic properties

The magnetic data have been collected on a powder sample of **2** checked by powder X-ray diffraction (Fig. S2). The thermal variation of the $\chi_M T$ product shows a monotonic increase from a room temperature value of 0.36 emu.K.mol⁻¹ to a 3 K value of 0.44 emu.K.mol⁻¹ (Fig. 3). This evolution indicates dominant ferromagnetic interactions between spin carriers. The $\chi_M T$ value stays close to the expected value for a non-coupled organic radical (0.375 emu.K.mol⁻¹) on a large range of temperatures, an indication that the ferromagnetic interaction is small. Following (i) the structural description at 293 K and (ii) the assumption that the exchange interaction is weak, the data are first fitted using a regular ferromagnetic spins 1/2 chain model e.g. with an exchange interaction parameter J that is independent of the temperature (see below). The high temperature expansion of the Heisenberg linear chain expression ($\mathcal{H} = -J \sum S_i S_{i+1}$) with Pade approximant¹⁵ was thus used to fit the data with a very good agreement between 10 and 300 K and an overestimation of the magnetic susceptibility at very low temperature. An additional mean field parameter was introduced in order to take into account the weaker interchain interactions⁷ leading to a very good agreement over the whole temperature range for an exchange parameter J of + 1.60 cm⁻¹ and a Curie Weiss temperature of -0.90 K (fig. 3).

Magneto-structural correlations

Two questions arise when comparing the structural and the magnetic studies: (i) why a temperature-independent J parameter ensure a good fit of the data whereas the XRD studies suggest that the interaction should vary with temperature? (ii) why do we observe a ferromagnetic exchange interaction whereas almost all the previously published verdazyl compounds led to an antiferromagnetic exchange interaction mediated by the π - π interactions?

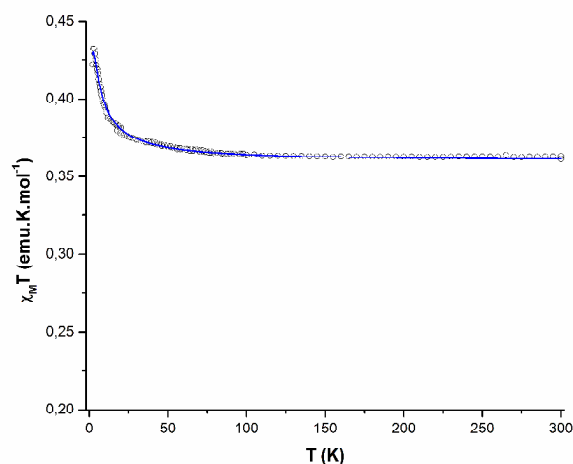


Fig. 3 Temperature dependence of the $\chi_M T$ product for **2**. The solid line is a fit to the Heisenberg linear chain expression for a regular ferromagnetic chain with $J = +1.60$ cm⁻¹ and $\Theta = -0.90$ K

The fact that a temperature-independent J parameter is sufficient to reproduce the magnetic behaviour of **2** is attributed to the weak value of the observed coupling. It thus becomes operant only in the low temperature region, on a limited range of temperature, where the relative structural variations are small. Accordingly, these variations cannot significantly influence the exchange interaction parameter which can thus be considered as constant.

Following Kahn's model,¹⁵ in order to understand the nature of the exchange interaction, the way the SOMOs of the radicals interact should be considered in the first place. The SOMO of the oxo-verdazyl radical is antibonding with nodes at the C(2) and C(6) atoms and significant contribution only on the N atoms.¹⁶ With the parallel displaced stacking observed in the structure, the atoms with high spin density of one radical are located in the nodal plane of the SOMO of the neighbouring radical. According to aforementioned model, this situation with no overlap between the SOMOs produces ferromagnetic interactions. To go beyond this qualitative approach, Robert *et al.*⁴ have systematically calculated the effect of slippages on the exchange interaction

between two verdazyl radicals. The authors thus predict that a slippage of 1.2 Å of one verdazyl ring along a direction parallel to the N(5) N(7) axis is enough to stabilize the triplet state. To our knowledge, **2** is the only example in the literature that allows to qualitatively verify this prediction. However, the value of the experimental exchange parameter remains well below the predicted values. The first reason for this discrepancy is that the authors have assumed an inter-radical distance of 3.2 Å, the one found in 1,1'-bis(verdazyl)ferrocene diradical¹⁷ whereas the one observed in **2** is much longer and, as stated earlier, this distance has a considerable influence on the J value. A second reason is related to an additional slippage along the main axis of the verdazyl radical that was not considered by Robert *et al.* This displacement leads to a decrease of the overlap density¹⁸ and hence of the exchange interaction parameter.

Despite the weak value of J, it remains that the slipped 1D chains obtained in **2** has guaranteed the obtention of the ferromagnetic interactions that were theoretically predicted. The absence of head over tail stacking, which has been previously observed and correlated with antiferromagnetic interactions in the case of 1,5-dimethyl-3-(aryl)-6-oxoverdazyl with aryl = imidazolyl,¹² pyridyl,² 2-hydroxyphenyl¹³ and 4-acetamidophenyl¹⁹ is striking, although the exact impact of the phenylethynyl substituent on the crystal packing remains an open question.

Conclusions

In this work, we have introduced a phenyl-ethynyl substituent on an oxo-verdazyl radical and strongly impacted the crystal packing which shows original 1D slipped π -stacks. This arrangement of the radicals leads to a rare case of ferromagnetic interactions between oxoverdazyl systems, in line with previous theoretical prediction. Starting from this unexpected results, further crystal engineering will be devoted to the realization of a molecular arrangement closer to the ideal slipped 1D chains described theoretically. This could be achieved through the disymmetrization of the N(3) and N(8) substituents, in order to increase the ferromagnetic interaction to a level at which a theoretical inspection becomes reasonable.

Experimental

Synthesis

1,5-dimethyl-3-(p-ethynylphenyl)-6-oxo-1,2,4,5-tetrazane 1 : 4-ethynyl-benzaldehyde (500 mg, 3.85 mmol, M = 130 g.mol⁻¹) was dissolved in 13 mL of methanol and added to a solution of bis(1-methylhydrazide) carbonic acid (454 mg, 3.85 mmol, M = 118 g.mol⁻¹) in 20 mL of methanol. The solution was refluxed for 15 hours and turned dark orange. The solvent was removed under reduced pressure and the residue was recrystallized in ethylacetate (18 mL) to give a colorless solid (499 mg, 2.17 mmol, M = 230 g.mol⁻¹) in 56 % yield. ¹H NMR (300 MHz, d⁶-DMSO): δ 7.57 (d, 1H, J = 8.1 Hz), 7.49 (d, 1H, J = 8.1 Hz), 5.76 (d, 2H, J = 7.0 Hz, NH), 4.95 (t, 1H, J = 7.0 Hz, CH), 4.19 (s, 1H, \equiv C-H), 2.93 (s, 6H, N-CH₃). ¹³C NMR (75 MHz, d⁶-DMSO): 154.9 (C=O), 138.3, 132.0, 127.9, 121.6, 83.7(\equiv C-), 81.4 (\equiv C-), 68.6 ((NH₂)₂CH), 38.1 (N-CH₃). FT-IR (KBr): 3250 (sh, ν (\equiv C-H)), 3225 ν (N-H), 2102 ν (C \equiv C), 1591 ν (C=O). Anal. Calcd for C₁₂H₁₄N₄O. 0.1 H₂O : C 62.11, H 6.17, N 24.14 %. Found C

61.95, H 6.05, N 23.65 %. HRMS (ESI+): m/z = 231.1249 (231.1246 for [M+H]⁺).

1,5-dimethyl-3-(p-ethynylphenyl)-6-oxoverdazyl 2 : Benzoquinone (173 mg, 1.60 mmol) was dissolved in 10 mL of toluene and added to a suspension of **1** (260 mg, 1.13 mmol) in 60 mL of toluene. The reaction mixture was refluxed for 15 min and a red solution was obtained. After cooling, a white precipitate (hydroquinone) was filtered off and the red solution was concentrated under reduced pressure. Column chromatography (SiO₂, CH₂Cl₂) afforded **2** (60 mg, 0.25 mmol) in 23 % yield. FT-IR (KBr): 3250 ν (\equiv C-H), 2102 ν (C \equiv C), 1684 ν (C=O). Anal. Calcd for C₁₂H₁₁N₄O: C 63.43, H 4.88, N 24.66 %. Found C 63.34, H 4.84, N 24.20. HRMS (ESI+): m/z = 227.0929 (227.0933 for [M]⁺). UV-vis λ_{\max} 425 nm (ϵ = 1557 mol⁻¹.L.cm⁻¹), λ_{\max} 483 nm ϵ = 471 mol⁻¹.L.cm⁻¹.

XRD

Single X-ray diffraction data have been collected on a selected red plate single crystal of **2** on a APEXII 4-circles diffractometer equipped with a Molybdenum monochromator (λ = 0.71073 Å). Diffraction data were collected with identical experimental conditions and on the single crystal at room temperature, 200K and 100K with the help of a Oxford Cryostream cryostat. Single crystal structures were solved by direct methods using the SIR97 program²⁰ and then refined with full-matrix least-square methods based of F².²¹ All non-hydrogen atoms were refined with anisotropic atomic displacement parameters and H atoms were finally included in their calculated positions after fine analysis of difference Fourier density maps.

X-ray diffraction pattern of a powder of **2** has been collected at room temperature using a Bruker AXS D8 Advance diffractometer equipped with a monochromatic CuK α 1 radiation (λ = 1.54056 Å) and a LynxEye detector. A small amount of pristine powder was put down on a disoriented silicon single crystal sample holder. Diffraction pattern profile analysis was performed with the help of the FullProf and WinPLOTR programs.²²

Magnetometry

Static magnetic susceptibility measurement was performed on a Quantum Design MPMS XL-5 system from 2 to 300 K at the field of 2000 Oe on several independently synthesized polycrystalline samples of **2** held in teflon tape. The high temperature slope of the $\chi_{\text{M}}T$ product has been corrected by the introduction of a TIP value of 1.77 10⁻⁴ emu.mol⁻¹. The linear Heisenberg model using the Pade approximant was used to analytically model the temperature dependence of the susceptibility.^{5b} A Curie Weiss temperature was introduced to take into account interchain interactions.¹⁵

Notes and references

^a UMR 6226 CNRS - Université de Rennes 1, Institut des Sciences Chimiques de Rennes, Campus de Beaulieu, F-35042 Rennes Cedex. Fax: +33 2 23 23 69 39; E-mail: lucie.norel@univ-rennes1.fr

^b LNCMI, UPR 3228, CNRS-UJF-UPS-INSA and UJF, 38042 Grenoble, France

† Electronic Supplementary Information (ESI) available: UV-vis spectrum and powder diffraction pattern, crystallographic data in cif format (CCDC 1012865-1012867). See DOI: 10.1039/b000000x/

- 1 (a) Ratera, I.; Veciana, J., *Chem. Soc. Rev.* **2012**, *41* (1), 303-349; (b) Hicks, R. G., *Org. & Biomol. Chem.* **2007**, *5* (9), 1321.
- 2 Jornet, J.; Deumal, M.; Ribas-Arino, J.; Bearpark, M. J.; Robb, M. A.; Hicks, R. G.; Novoa, J. J., *Chem. Eur. J.* **2006**, *12* (15), 3995.
- 3 Norel, L.; Rota, J. B.; Chamoreau, L. M.; Pilet, G.; Robert, V.; Train, C., *Angew Chem.Int. Ed.* **2011**, *50* (31), 7128.
- 4 Rota, J. B.; Le Guennic, B.; Robert, V., *Inorg. Chem.* **2010**, *49* (3), 1230.
- 5 (a) Constantinides, C. P.; Koutentis, P. A.; Rawson, J. M., *Chem. Eur. J.* **2012**, *18* (23), 7109. (b) Yan, B.; Cramen, J.; McDonald, R.; Frank, N. L., *Chem. Commun.* **2011**, *47* (11), 3201.
- 6 (a) Chiarelli, R.; Novak, M. A.; Rassat, A.; Tholance, J. L., *Nature* **1993**, *363*, 147. (b) Caneschi, A.; Ferraro, F.; Gatteschi, D.; Le Lirzin, A.; Novak, M. A.; Rentschler, E.; Sessoli, R. *Adv. Mater* **1995**, *476*, 478.
- 7 (a) Koivisto, B.D., Hicks, R.G., *Coord. Chem. Rev.* **2005**, *249*, 2612. (b) Train, C.; Norel, L.; Baumgarten, M., *Coord. Chem. Rev.* **2009**, *253* (19-20), 2342.
- 8 (a) Mukai, K.; Kawasaki, S.; Jamali, J. B.; Achiwa, N., *Chem. Phys. Lett.* **1995**, *241* (5-6), 618; (b) Mukai, K.; Nuwa, M.; Morishita, T.; Muramatsu, T.; Kobayashi, T. C.; Amaya, K., *Chem. Phys. Lett.* **1997**, *272* (5-6), 501-505; (c) Mukai, K.; Nuwa, M.; Suzuki, K.; Nagaoka, S.; Achiwa, N.; Jamali, J. B., *J. Phys. Chem. B* **1998**, *102* (5), 782.
- 9 (a) Allemand, P. M.; Srdanov, G.; Wudl, F., *J. Am. Chem. Soc.* **1990**, *112* (25), 9391. (b) Mito, M.; Takeda, K.; Mukai, K.; Azuma, N.; Gleiter, M.R.; Krieger, C.; Neugebauer, F. A. *J. Phys. Chem. B* **1997**, *101*, 9517.
- 10 (a) Di Piazza, E.; Norel, L.; Costuas, K.; Bourdolle, A.; Maury, O.; Rigaut, S., *J. Am. Chem. Soc.* **2011**, *133*, 6174; (b) Meng, F. B.; Hervault, Y. M.; Shao, Q.; Hu, B. H.; Norel, L.; Rigaut, S.; Chen, X. D., *Nat. Comm.* **2014**, *5*, 9. (c) Norel, L.; Feng, M.; Bernot, K.; Roisnel, T.; Guizouarn, T.; Costuas, K.; Rigaut, S., *Inorg. Chem.* **2014**, *53*, 2361.
- 11 Chemistruck, V.; Chambers, D.; Brook, D. J. R., *J. Org. Chem.* **2009**, *74* (5), 1850.
- 12 Norel, L.; Pointillart, F.; Train, C.; Chamoreau, L. M.; Boubekeur, K.; Journaux, Y.; Brieger, A.; Brook, D. J. R., *Inorg. Chem.* **2008**, *47* (7), 2396.
- 13 Norel, L.; Chamoreau, L. M.; Train, C., *Polyhedron* **2010**, *29* (1), 342-348.
- 14 Verot, M.; Brefuel, N.; Pecaut, J.; Train, C.; Robert, V., *Chem. Asian J.* **2012**, *7* (2), 380.
- 15 Kahn, O., *Molecular Magnetism*. Wiley-VCH Verlag GmbH: Weinheim: Germany, 1993.
- 16 Rota, J. B.; Norel, L.; Train, C.; Ben Amor, N.; Maynau, D.; Robert, V., *J. Am. Chem. Soc.* **2008**, *130* (31), 10380.
- 17 Koivisto, B. D.; Ichimura, A. S.; McDonald, R.; Lemaire, M. T.; Thompson, L. K.; Hicks, R. G., *J. Am. Chem. Soc.* **2006**, *128* (3), 690.
- 18 Verdaguer, M.; Bleuzen, A.; Marvaud, V.; Vaissermann, J.; Seuleiman, M.; Desplanches, C.; Scuille, A.; Train, C.; Garde, R.; Gelly, G.; Lomenech, C.; Rosenman, I.; Veillet, P.; Cartier, C.; Villain, F., *Coord. Chem. Rev.* **1999**, *192*, 1023.
- 19 Plater, M. J.; Kemp, S.; Coronado, E.; Gomez-Garcia, C. J.; Harrington, R. W.; Clegg, W. *Polyhedron* **2006**, *25*, 2433.
- 20 Altomare, A.; Burla, M. C.; Camalli, M.; Cascarano, G. L.; Giacovazzo, C.; Guagliardi, A.; Moliterni, A. G. G.; Polidori, G.; Spagna, R., *J. App. Cryst.* **1999**, *32*, 115.
- 21 Sheldrick, G. M., *Acta Cryst. Section A* **2008**, *64*, 112.
- 22 (a) Roisnel, T.; Rodriguez-Carvajal, J., *Epdic 7: European Powder Diffraction, Pts 1 and 2* **2001**, *378-3*, 118-123; (b) Rodriguez-carvajal, J., *Phys. B* **1993**, *192* (1-2), 55.

70

The newly synthesized *p*-ethynylphenyl-oxoverdazyl radical show unusual slipped 1D chains held together by π - π interactions leading to ferromagnetic exchange interactions.

